

## Mesostructural Evolution of Iron Oxide-SDS Composites: A TEM and PXRD Study

FEIHU LI<sup>1,2,\*</sup> and DONGYANG NIE<sup>1</sup>

<sup>1</sup>School of Environmental Science and Engineering, Nanjing University of Information Science and Technology, Jiangsu Engineering Technology Center for Environmental Purification Materials Research; Jiangsu Key Lab of Atmospheric Environment Monitor and Pollution Control, Nanjing 210044, P.R. China

<sup>2</sup>Current address: Earth Science Division, Lawrence Berkeley National Laboratory, Berkeley, California 94720, United States of America

\*Corresponding author: Tel/Fax: +86 25 58731090, E-mail: favorlee@163.com

Received: 20 June 2013;

Accepted: 4 November 2013;

Published online: 10 May 2014;

AJC-15141

In present study, we synthesized iron oxide-sodium dodecyl sulfonate (SDS) composites by using a solvothermal route (ethyl alcohol-water) and demonstrated that the iron oxide-SDS composites undergo a mesostructural transition from lamellar to hexagonal as a function of ageing time. With increasing ageing time, the composite mesostructure evolved from a regular lamellar symmetry to a transitional lamellar-hexagonal symmetry and eventually to an ordered hexagonal symmetry with a unit cell parameter of  $a = 44 \text{ \AA}$ . The direct evidences of mesostructural evolution were acquired from transmission electron microscopy and further confirmed by powder X-ray diffraction. A lamellar-to hexagonal transition mechanism was proposed to explain the mesostructural transition of iron oxide-SDS composites.

**Keywords:** Iron oxides, Sodium dodecyl sulfonate, Mesostructural transition, Lamellar-to-hexagonal.

### INTRODUCTION

Since the first report of ordered mesoporous silicates<sup>1</sup>, increasing attention has focused on the synthesis of self-assembled inorganic-surfactant composites—especially mesostructured metal oxide-surfactant composites<sup>2-4</sup>—probably due to their potential applications as catalysts and absorbents. The synthetic routes of mesostructured biphasic composites are heavily precursor-dependent<sup>2</sup>, *i.e.*, anionic precursor species ( $\Gamma^-$ ) are expected to react with cationic surfactant ( $S^+$ ), following the direct  $S^+\Gamma^-$  route to form an  $S^+\Gamma^-$  complex, for example, order mesoporous silica MCM-41 was prepared by reaction of cationic CTAB with anionic siliceous species<sup>1</sup>. Whereas cationic precursors ions preferably react with anionic surfactant to form  $S^-\Gamma^+$  complex, further removal of surfactant will produce mesoporous metal oxides. For example, hexagonal mesoporous PbO has been synthesized by reaction of alkyl sulfonate with lead ions<sup>2</sup>. Yada and coworkers<sup>5</sup> also reported that hexagonal mesoporous  $\text{Al}_2\text{O}_3$  can be prepared by homogeneous precipitation of sodium dodecyl sulfate (SDS) and aluminum ions in the presence of urea.

Iron oxides have been widely used in dyes, magnetic devices, catalysts and rechargeable lithium batteries<sup>6</sup>. Porous iron oxides, especially mesoporous iron oxides has attracted considerable attentions because of their easily accessible

mesopores and good kinetic performance<sup>7,8</sup>. Mesostructured iron oxides have been prepared by using either organic surfactants as structure-directing agents (SDAs), typically cationic surfactant ( $S^+$ ) for  $S^+\Gamma^-$  routes<sup>7-9</sup>, or ordered mesoporous silica as hard templates<sup>10-12</sup>. The first attempt to prepare mesostructured iron oxides *via*  $S^+\Gamma^-$  route was performed by Huo *et al.*, but only lamellar mesophase was achieved<sup>2</sup>. Using aliphatic alcohols as synthetic solvent and sodium hexadecylsulfonate (typical  $S^-$ ) as structure-directing agent, Michot *et al.*<sup>13</sup> first demonstrated MCM-like, *i.e.*, hexagonal mesostructured iron oxides can be prepared *via*  $S^+\Gamma^-$  method. On the other hand, it has been reported that the mesophase of lamellar PbO will transform to hexagonal by varying the molar ratio of surfactant to inorganic species and/or the pH of the starting mixture<sup>2</sup>. Yada *et al.*<sup>14</sup> also observed similar mesophase evolutions in some rare-earth metal oxide-surfactant systems, such as Ho, Tm, Yb, Gd, Lu and Er-based-surfactant mesophases. Besides, the mesophases transition from lamellar to hexagonal was also verified for aluminum-SDS composites<sup>15</sup>. The transition of mesophase is of great importance for both fundamental understanding the mesostructure evolution during the preparing process and the development of novel mesostructured materials with tailorable pore configurations<sup>16,17</sup>. It is supposed that mesostructured metal oxide-surfactant composites would proceed structure transition between different configurations

by varying the synthetic parameters, if there are more than one type of configurations of the employed surfactants. Both regular lamellar and hexagonal iron oxide-SDS mesostructures have been reported recently<sup>4,13</sup>. However, there is not enough evidence to prove whether the iron oxide-SDS composites undergo mesostructural transition between the two configurations. Moreover, the underlying mechanism of the transition of diphasic mesostructured composites is not so well understood. Only a few studies have addressed the transition of mesophases<sup>2,15</sup>, with a special emphasis on silica-based mesoporous materials to understand the effects of synthetic parameters on the transition of these mesophases<sup>16,18,19</sup>.

Herein, we synthesized mesostructured iron oxide-SDS composites in an EtOH-H<sub>2</sub>O solution and monitored their mesophase transition by both powder X-ray diffraction (PXRD) and transmission electron microscopy (TEM). Our objective is to better understand the mesostructural evolution of the iron oxide-SDS composites and the underlying mechanism governing the mesostructural transition process.

## EXPERIMENTAL

All chemicals were purchased from Sinopharm Chemical Reagent Co., Ltd (Shanghai, China) and used without further purifications. Anhydrous ferric chloride (FeCl<sub>3</sub>) was used as the iron source and sodium dodecyl sulfonate (SDS, C<sub>12</sub>H<sub>25</sub>NaO<sub>3</sub>S (Fig. 1) was employed as the structure-directing agent. Absolute ethyl alcohol (EtOH) and Milli-Q ultrapure water were used as synthetic solution.

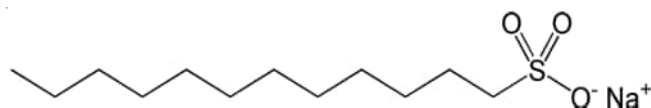


Fig. 1. Chemical structure of sodium dodecyl sulfonate (SDS)

**Preparation of iron oxide-SDS composite:** Typically, the iron oxide-SDS composite was prepared as follows: firstly, 6 mmol of ferric chloride was added dropwise in a 10 mL of 0.3 M NaOH solution and prehydrolyzed for 10 min before mixing with a 40 mL of 0.3 M SDS in absolute ethyl alcohol solution. Then, the resultant suspension (pH = 1.75) was magnetically stirred and intermittently sonicated at 40 °C for 1 h followed by transferring to sealed polypropylene bottles and ageing at 80 °C for 6, 24 and 72 h, respectively. The final product was cooled to ambient temperature, recovered by vacuum filtration and washed with excessive EtOH for several times and air-dried for further test.

**Characterization:** Transmission electron microscopy (TEM) was carried out using a JEOL JEM-4000EX microscope. A drop of ethanol suspension containing composite samples with different ageing times was applied to a copper grid (300 mesh) coated with carbon film. The copper grid was allowed to dry in air then ready for TEM analysis operated at 400 keV for high-resolution imaging. Powder X-ray diffraction (PXRD) measurements were performed on an ARL X'TRA diffractometer with CuK<sub>α</sub> radiation (Operating power: 40 kV, 40 mA). To prepare samples for PXRD analyses, a small spoon of sample was grinded and then supported in a square groove on a flat sheet of glass and flattened prior to tests. Powder X-

ray diffraction data were collected in the 2θ range of 1-10° with a scanning rate of 1°/min.

## RESULTS AND DISCUSSION

**Transmission electron microscopy:** TEM images of the iron oxide-SDS composites with different ageing time (Fig. 2) provide a visible and ex-situ mesostructural evolution process that the composites experienced. With the ageing time increased, the mesostructure of the composites transitioned from the regular lamellar frame work (Fig. 2a) to an interim poor-ordered

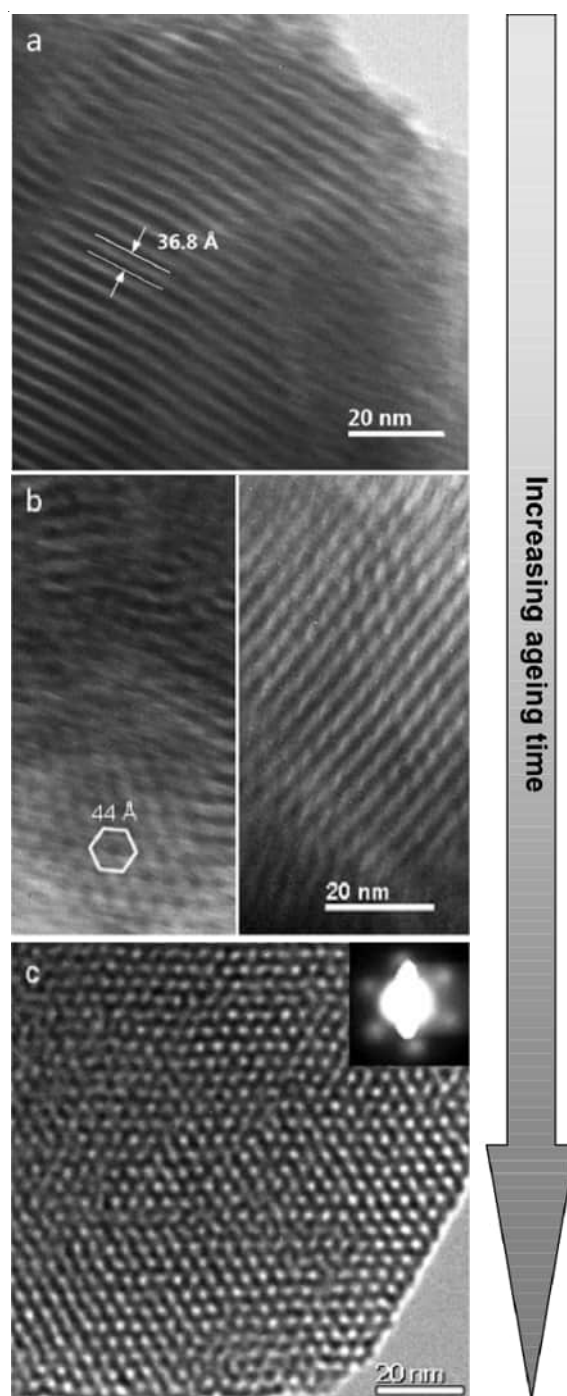


Fig. 2. TEM images of the iron oxide-SDS composites showing the mesostructural evolution of the composites with increasing ageing time: (a) 6 h, (b) 24 h, (c) 72 h (inset: corresponding selected area electron diffractogram)

hexagonal array with a unit cell parameter of  $a = 44 \text{ \AA}$  (Fig. 2b) and finally to the well-ordered hexagonal structure (Fig. 2c). The hexagonal ordering was verified by the selected area electron diffractogram (inset in Fig. 2c). Similar transition from lamellar to worm-like mesostructure was also observed by TEM for titanium dioxide-surfactant matrix<sup>20</sup>. Using TEM technology, Liang *et al.* have also shown obvious mesostructure transitions of periodic mesoporous organosilicas with changing the concentration of sodium hydroxides in the starting mixture<sup>17</sup>.

**Powder X-ray diffraction:** Powder XRD patterns of these iron oxide-SDS composites are shown in Fig. 3. Ageing the starting iron oxide-SDS mixture for 6 h resulted in a composite with a XRD pattern characterized by three diffraction peaks at  $2\theta = 2.4, 4.8, 7.2^\circ$  (Fig. 3, bottom). The peaks can be assigned to (001), (002) and (003) reflections of a layered phase with an interlayer spacing ( $d_{(001)}$ ) of  $36 \text{ \AA}$ , in good agreement with TEM result of  $36.8 \text{ \AA}$  as shown in Fig. 2a. Moreover, it's reported that the layer  $d$  spacing of iron oxide-surfactant composites are directly proportional to the surfactant carbon chain length<sup>4</sup> and that the  $d_{(001)}$  spacing of layer iron oxide-surfactant composite made with a 12-carbon sulfate surfactant equals to  $36.6 \text{ \AA}$ , which is in good consistence with our results.

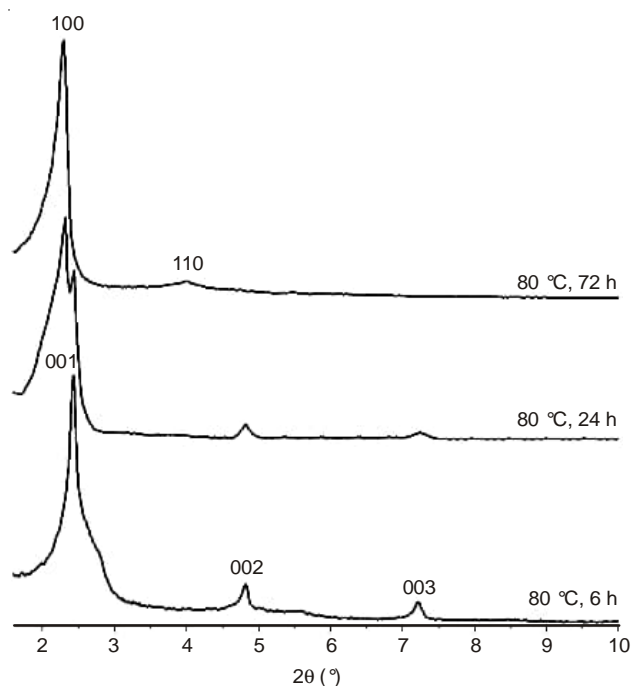


Fig. 3. Powder XRD patterns of the iron oxide-SDS composites

When the ageing time was prolonged to 24 h, the powder XRD pattern of the composite (Fig. 3, middle) shows a bi-peak with  $d$  spacing of  $38$  and  $36 \text{ \AA}$  [assigned to (001) reflection] in the  $2\theta$  angle and two decreased peaks corresponding to (002) and (003) reflections of the lamellar composite, implying that the layered mesostructure remained upon ageing for 24 h. This observation is probably due to the formation of a cross-linked iron oxy-hydroxide layer at this stage<sup>4</sup>. The diffraction peak with  $d$  spacing of  $38 \text{ \AA}$  can be assigned to the (100) reflection of a poorly-ordered hexagonal mesostructure with a unit cell parameter of  $a = 44 \text{ \AA}$  (calculated from formula  $a = 2d_{100}/\sqrt{3}$ ). The calculated unit cell parameter is coincident with TEM result as depicted in Fig. 2b. Combination the TEM observations (Fig. 2b) and the PXRD results (Fig. 3, middle) suggests that co-occurring of both lamellar and hexagonal mesostructures of the iron oxide-SDS composites after ageing for 24 h. In fact, co-occurring of two mesophases have also been reported for Er-based mesophases<sup>14</sup> and mesostructured aluminophosphates<sup>21</sup>. With further increase in ageing time up to 72 h, the layered mesophase disappeared, while only a second mesophase was obtained with two clear peaks attributable to (100) and (110) reflections (Fig. 3, top) assignable to a hexagonal symmetry as described above, in consistent with the TEM analysis (Fig. 2c). Further increase in ageing time didn't affect the positions of these diffraction peaks (data not shown), implying formation of relative stable hexagonal iron oxide-SDS composites.

**Proposed mechanism:** On the basis of above TEM and PXRD analyses, a schematic mechanism in agreement with our experimental observations was proposed to illuminate the lamellar-to-hexagonal transition (Fig. 4). In the initial step, SDS surfactants tend to form a bilayer configuration in the interlayers of layered iron oxide planes consist of  $\text{Fe}(\text{H}_2\text{O})_6^{3+}$  octahedral units. This layered configuration has been already confirmed<sup>22</sup> with increasing ageing time, the SDS surfactant anions undergo cylindrical micellization due to the change of the solution pH and therefore the interfacial forces between the surfactant surface and iron oxide sheets. This process along with the polymerization of iron aquo complex lead to the corrugation of the layered surfactant-iron oxide sheets. As depicted in Fig. 4, this process proceeds steadily until the cross-linking between two adjacent sheets at the contacted area, finally resulting in the formation of hexagonal iron oxide-SDS mesostructure.

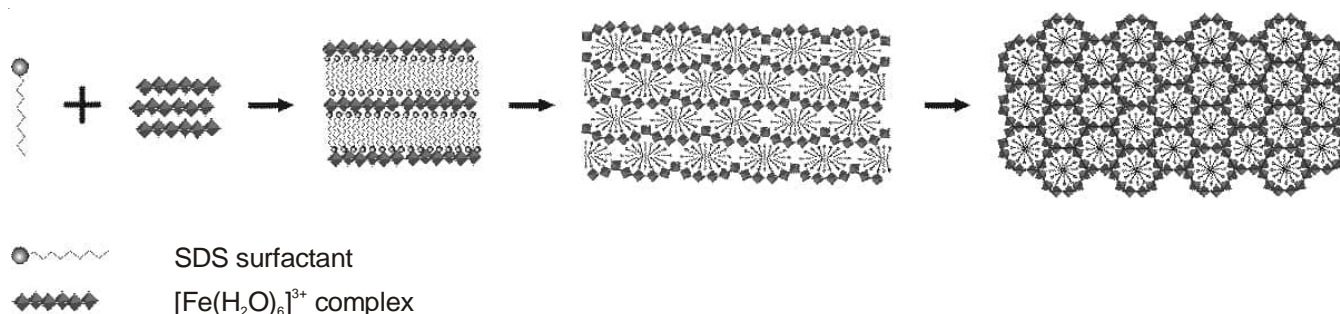


Fig. 4. Schematic diagram of mechanism proposed for the lamellar-to-hexagonal transition of iron oxide-SDS composites

Actually, a similar mechanism was reported for the silica-based mesophase<sup>19</sup> and for the aluminum-based surfactant mesophase<sup>15</sup>. The driving force of the lamellar-to-hexagonal transition seems to be the balance between the condensation of iron oxide complex and the interfacial electrostatic interaction, both of which are strongly correlated to the pH and the parent solvent components<sup>13,15</sup>. The introduction of EtOH into the starting mixture seems to play a significant role in the lamellar-to-hexagonal transition of iron oxide-SDS mesophase, by which the parameter that determines the preferred configuration of a surfactant assembly was likely to be in the range favoring the formation of cylindrical micelles<sup>2,19</sup>. In this respect, the preferred configuration of the a surfactant system ultimately governs the mesostructure evolution of iron oxide-SDS composites, this is also true for mesophase templated by non-ionic SDAs<sup>23</sup>.

### Conclusion

In summary, both TEM and powder XRD evidences of lamellar-to-hexagonal transition of mesostructured iron oxide-SDS composite were presented in current work. The mesophase evolution of iron oxide-SDS composites from lamellar to hexagonal symmetry was obtained by introduction of ethyl alcohol into the starting mixture, followed by ageing the mixture at 80 °C and extending the ageing time from 6 to 72 h. Results of TEM and powder XRD suggest that iron oxide-SDS composite mesostructurally evolved from a regular lamellar symmetry to a transitional lamellar-hexagonal symmetry and eventually to an ordered hexagonal symmetry with a unit cell parameter of  $a = 44 \text{ \AA}$ . As implied by the proposed lamellar-to-hexagonal transition mechanism, the mesostructural evolution process is governed by the preferred configuration of SDS surfactant system, which is dependent on both pH and the solvent components. This lamellar-to-hexagonal transition will be possible for other transition metal oxide-surfactant composites, especially those prepared in a alcohol-water system.

### ACKNOWLEDGEMENTS

This work has been funded in part by NSFC (Grant Nos. 51002080, 5131 0105009), CSC (Grant No. 2011832032) and the Priority Academic Program Development of Jiangsu Higher

Education Institutions. We would like to thank Prof. J. M. Zhu at Nanjing University for TEM studies.

### REFERENCES

1. C.T. Kresge, M.E. Leonowicz, W.J. Roth, J.C. Vartuli and J.S. Beck, *Nature*, **359**, 710 (1992).
2. Q.S. Huo, D.I. Margolese, U. Ciesla, D.G. Demuth, P.Y. Feng, T.E. Gier, P. Sieger, A. Firouzi and B.F. Chmelka, *Chem. Mater.*, **6**, 1176 (1994).
3. D.M. Antonelli, A. Nakahira and J.Y. Ying, *Inorg. Chem.*, **35**, 3126 (1996).
4. S.H. Tolbert, P. Sieger, G.D. Stucky, S.M.J. Aubin, C.C. Wu and D.N. Hendrickson, *J. Am. Chem. Soc.*, **119**, 8652 (1997).
5. M. Yada, M. Machida and T. Kijima, *Chem. Commun.*, 769 (1996).
6. R.M. Cornell and U. Schwertmann, *The Iron Oxides: Structure, Properties, Reactions, Occurrences and Uses*, Wiley-VCH Verlag GmbH & Co. KGaA, Weinheim, FRG, edn 2, Chap. 1, pp. 1-7 (2004).
7. D.N. Srivastava, N. Perkas, A. Gedanken and I. Felner, *J. Phys. Chem. B*, **106**, 1878 (2002).
8. A.S. Malik, M.J. Duncan and P.G. Bruce, *J. Mater. Chem.*, **13**, 2123 (2003).
9. F. Jiao and P.G. Bruce, *Angew. Chem. Int. Ed.*, **43**, 5958 (2004).
10. F. Jiao, A. Harrison, J.C. Jumas, A.V. Chadwick, W. Kockelmann and P.G. Bruce, *J. Am. Chem. Soc.*, **128**, 5468 (2006).
11. F. Jiao, J.C. Jumas, M. Womes, A.V. Chadwick, A. Harrison and P.G. Bruce, *J. Am. Chem. Soc.*, **128**, 12905 (2006).
12. F.H. Li, X.R. Fu, J. Huang and J.P. Zhai, *Chem. Res. Chin. Univ.*, **28**, 559 (2012).
13. L.J. Michot, C. Mathieu and E. Bouquet, *C. R. Acad. Sci. Ser. IIC Chim.*, **1**, 167 (1998).
14. M. Yada, H. Kitamura, A. Ichinose, M. Machida and T. Kijima, *Angew. Chem. Int. Ed.*, **38**, 3506 (1999).
15. M. Yada, H. Hiyoshi, K. Ohe, M. Machida and T. Kijima, *Inorg. Chem.*, **36**, 5565 (1997).
16. Y.F. Zhao, D.L. Zhang, L. Zhao, G.C. Wang, Y.H. Zhu, A. Cairns, J.L. Sun, X.D. Zou and Y. Han, *Chem. Mater.*, **23**, 3775 (2011).
17. Y.C. Liang, E.S. Erichsen, M. Hanzlik and R. Anwender, *Chem. Mater.*, **20**, 1451 (2008).
18. S.B. Jung, T.J. Ha and H.H. Park, *J. Colloid Interf. Sci.*, **320**, 527 (2008).
19. A. Monnier, F. Schuth, Q.S. Huo, D. Kumar, D. Margolese, R.S. Maxwell, G.D. Stucky, M. Krishnamurty, P. Petroff, A. Firouzi, M. Janicke and B.F. Chmelka, *Science*, **261**, 1299 (1993).
20. D.H. Wang, Z. Ma, S. Dai, J. Liu, Z.M. Nie, M.H. Engelhard, Q.S. Huo, C.M. Wang and R. Kou, *J. Phys. Chem. C*, **112**, 13499 (2008).
21. P.Y. Feng, Y. Xia, J.L. Feng, X.H. Bu and G.D. Stucky, *Chem. Commun.*, 949 (1997).
22. S.H. Tolbert, A. Firouzi, G.D. Stucky and B.F. Chmelka, *Science*, **278**, 264 (1997).
23. G.D. Stucky, P. Yang, D. Zhao, D.I. Margolese and B.F. Chmelka, *Nature*, **396**, 152 (1998).